Morphogenesis of calcitic sponge spicules: a role for specialized proteins interacting with growing crystals

J. AIZENBERG,*·[1] J. HANSON,[†] M. Ilan,** L. LEISEROWITZ,[‡] T. F. KOETZLE,[†] L. ADDADI,*·[1] AND S. WEINER*

*Departments of Structural Biology and [‡]Materials and Interfaces, Weizmann Institute of Science, Rehovot, Israel; Department of Zoology, Tel Aviv University, Tel Aviv, Israel; and [†]Chemistry Department, Brookhaven National Laboratory, Upton, New York, USA

ABSTRACT **Crystals formed in biological tissues often adopt remarkable morphologies that are thought to be determined mainly by the shapes of the confined spaces in which they grow. Another possible way of controlling crystal shape, demonstrated only in vitro, is by means of specialized proteins preferentially interacting with certain crystal faces. In so doing, they reduce the rate of growth in these directions and consequently change the overall crystal shape. In an X-ray diffraction study of the distribution of defects within the lattice of calcite crystals produced by certain sponges, we show that a remarkable correlation exists between the defect patterns or crystal texture and the macroscopic morphology of the spicules. This was observed in two cases in which proteins are present within the spicule crystal, but not in a third case where such intracrystalline proteins are absent. Furthermore, one of the spicules exhibited marked differences in texture even within families of structurally identical crystal planes, demonstrating that the organisms exert exquisite control over the microenvironment in which crystals grow. We conclude that highly controlled intercalation of specialized proteins inside the crystals is an additional means by which organisms control spicule growth.—Aizenberg, J., Hanson, J., Ilan, M., Leiserowitz, L., Koetzle, T. F., Addadi, L., Weiner, S. Morphogenesis of calcitic sponge spicules: a role for specialized proteins interacting with growing crystals. *FASEB J.* 9, 262–268 (1995)**

Key Words: biomineralization · calcisponges · X-ray diffraction · calcite · crystal morphology

BIOLOGICALLY FORMED MINERALS EXHIBIT an exquisite variety of shapes that are usually quite different from their inorganic counterparts. In general, the shapes of biogenic crystals are thought to be determined by the confined spaces in which they are induced to form (1). These spaces are delineated either by membranes in the form of vesicles, syncitia, or tightly adhering cells or by self-assembling arrays of specialized macromolecules (2–4). Specialized acidic proteins are also found in almost all tissues, in which control is exerted over mineral formation. They are intimately associated with the surface of the biogenic minerals, and are also present within the mineral phase itself. They are widely thought to be among the key components active in controlling crystal formation (5).

Proteins extracted from within biogenic calcitic skeletal elements are able to alter the morphology of crystals grown in vitro by preferentially interacting from solution with certain crystal faces, and consequently reducing the rate of growth in the corresponding directions. The adsorbed proteins are overgrown by the crystal and become occluded on particular planes within the crystal itself (6, 7). Local release of intracrystalline macromolecules from cleaned calcitic skeletons during slow epitaxial overgrowth of new calcite crystals on the skeletal surfaces also results in modified calcite morphologies (8).

The intracrystalline proteins create and stabilize discontinuities in the crystal lattice, and hence reduce the degree of perfection of the material, i.e., affect crystal texture. This effect can be quantitatively evaluated by using high-resolution X-ray diffraction to measure the average distance between produced imperfections in a given direction. This distance is known as the coherence length. X-ray diffraction can also be used to determine the extent to which microdomains of perfect lattice structure are misaligned relative to each other. This is known as the angular dispersion or angular spread, and in its reciprocal form we refer to it as the degree of alignment (9, 10).

The variations in coherence length observed in certain echinoderm and mollusk calcite crystals are consistent with the control over texture being mainly exerted by the occluded proteins. This was inferred from the fact that the greatest reduction in coherence lengths occurred in directions perpendicular to the crystal planes on which macromolecules specifically adsorbed in vitro (10). We also noted that the directions of elongation of the macroscopic skeletal elements coincide with longer coherence lengths in the same direction, and vice versa (11). This unexpected observation raised the interesting question as to whether a well-defined relation really exists between protein intercalation, revealed by the anisotropy in crystal textural properties, and the macroscopic morphologies of the single crystalline skeletal elements.

To investigate this phenomenon, we studied spicules of calcisponges. They have a wide variety of morphologies (12), and yet each is a single crystal of calcite (13). The spicules form in an extracellular membrane-bound compartment that is surrounded by cells connected to each other by septate junctions (14). The specific gravities of the spicules are slightly less than that of pure calcite, and they usually contain significant amounts of magnesium (15). Many, but not all, of the spicules cleave with a conchoidal fracture rather

[1]To whom correspondence should be addressed, at: Department of Structural Biology, Weizmann Institute of Science, Rehovot 76100, Israel.

[2]Crystal planes are denoted by a set of Miller indices, *h, k, l,* which define their orientation relative to the crystal axes. For calcite, for example, the {012} family contains the symmetry related equivalent (012), ($\bar{1}$02), and (1$\bar{1}$2) crystallographic planes. [012] denotes the direction of the diffraction vector perpendicular to the (012) plane.

[3]Abbreviations: DDW, double-distilled water; SEM, scanning electron microscope; CL, coherence length.

0892-6638/95/0009-0262/$01.50.

than the smooth fracture characteristic of pure calcite. It has been surmised that some of these properties are due to the presence of organic matter inside the spicules (16). One of their most interesting properties for our purposes is that for each spicule type the orientations of the crystallographic axes are always related in a constant manner to its morphology, but that different-shaped spicules may have differently oriented crystallographic axes (17).

Figure 1 shows the three spicule types we discuss here of the six types investigated. For comparison, a synthetically grown crystal of pure calcite is also shown (Fig. 1*A*). *Clathrina* forms one basic spicule type, namely planar equiangular triradiates about 100 μm across (Fig. 1*B*). They are well embedded within the tissue. The *c* crystallographic axis is oriented perpendicular to the plane of the spicule and the a^* axes coincide with the directions of the rays (12). As to the hypothesis that occluded proteins are involved in determining spicule shape, we would expect a reduction in coherence length in the direction of the *c* axis, relative to coherence lengths in the *ab* plane, and in synthetic calcite.

Sycon forms four different-shaped spicules: two forms of triradiates, one quadriradiate, and two forms of monaxons (18). Here we studied the two monaxon types, namely the slender monaxon and the curved monaxon. The former are very long (up to a few millimeters) and thin ($\sim$4 μm), and are extremely fragile (Fig. 1*C*). They are concentrated around the osculum in such a way that almost 90% of each spicule protrudes from the tissue. The *c* crystallographic axis is aligned with the spicule morphological axis (17). We therefore expect that the coherence lengths in the *ab* plane should

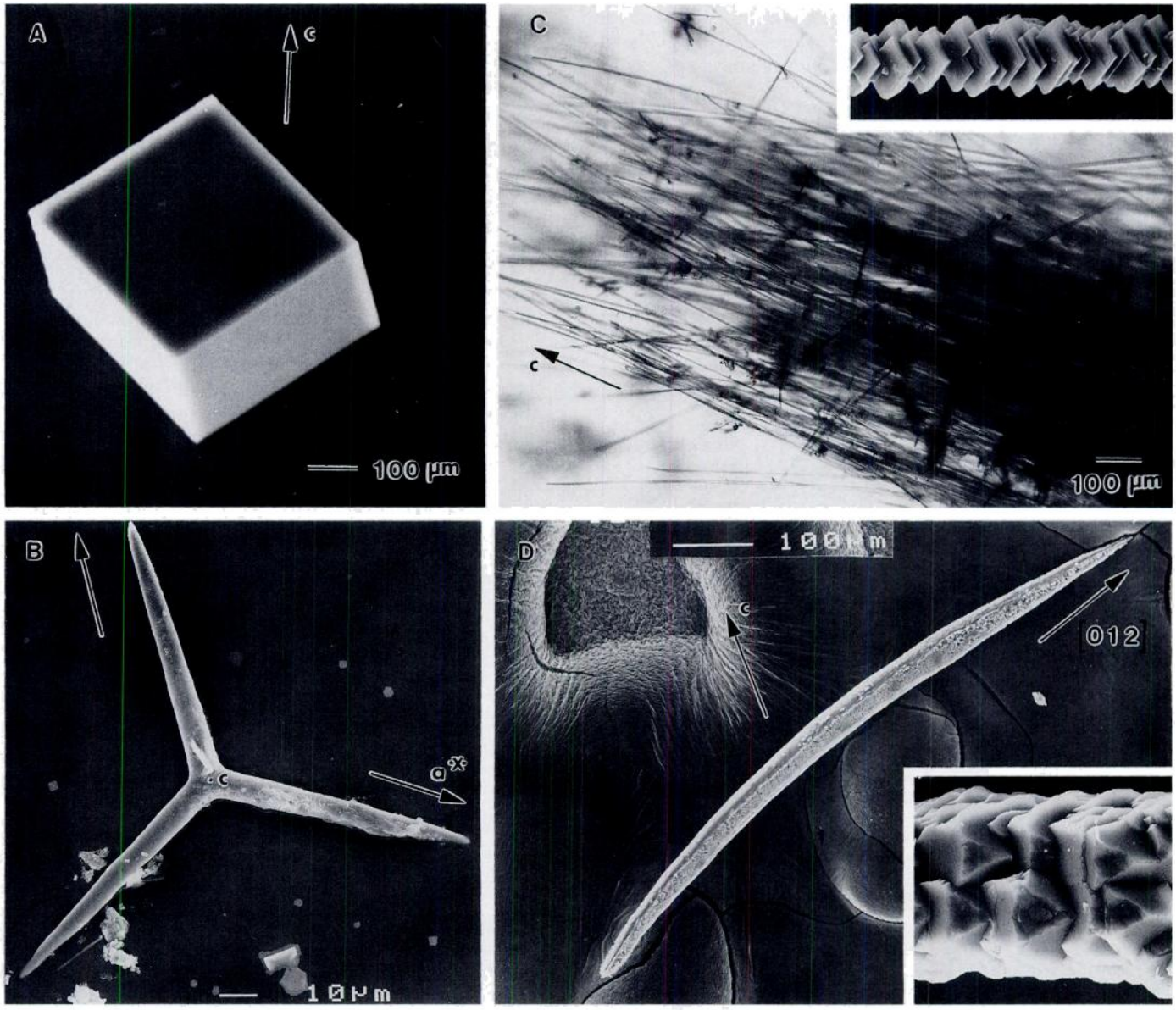

Figure 1. Scanning electron micrographs of the synthetic calcite crystal and spicules studied. *A)* Synthetic calcite crystal grown in the absence of additives. Only the stable {104} hexagonal faces are expressed. *B)* Spicules from the calcareous sponge *Clathrina sp.* The spicules are all planar equiangular triradiates and their crystallographic axes directions are shown. *C)* Slender monaxons (light micrograph) from the calcareous sponge *Sycon sp.* The spicules are elongated along the *c* axis. Insert: New calcite crystals grown epitaxially by slow diffusion on a cleaned slender monaxon. *D)* Curved monaxon spicules from *Sycon sp.* They grow roughly along the [012] direction, and are restricted in the symmetry related [$\bar{1}$02]- and [1$\bar{1}$2]-directions. Insert: New calcite crystals grown epitaxially by slow diffusion on a cleaned curved monaxon.

be reduced relative to that along the *c* axis.

The *Sycon* curved monaxons are about 1 mm long and 50 μm thick. Only a small proportion of the spicule emerges out of the tissue. The *c* axis is oriented at a constant angle of about 70° in relation to the approximate main direction of elongation of the spicule, which is roughly between the [011] and [012] directions[2] (Fig. 1*D*). The macroscopic morphology of this spicule does not respect the hexagonal crystallographic symmetry of calcite (17). It is thus particularly interesting to investigate whether and how the biological environment can overcome the intrinsic crystallographic symmetry of the material.

We show here that the textural properties of the slender monaxons and synthetic calcite are very similar, despite major differences in morphology. We also show that for the triradiates and curved monaxons there is a very clear correlation between spicule morphology and crystal texture. The results strongly suggest that the intracrystalline proteins are involved in determining the shape of the growing crystals, and that this process is exquisitely controlled.

MATERIALS AND METHODS

Collection and Preparation of the Material

Calcareous sponges *Clathrina sp.* and *Sycon sp.* (eastern Mediterranean) were collected, washed with fresh water, and rapidly frozen in liquid nitrogen in order to avoid subsequent dissolution or crystallization of calcium carbonate. After thawing, the tissues were treated with 2.5% sodium hypochloride solution on a rocking table for 1 h. The spicule suspension was then rinsed several times with double-distilled water (DDW)[3] and the cleaned spicules were air-dried. Examination in the scanning electron microscope (SEM) showed little or no evidence of etching.

Extraction of Intracrystalline Macromolecules

Clean, dry spicules of different shapes were suspended in DDW and decalcified by addition of stoichiometric amounts of concentrated HCl. The solution was then exhaustively dialyzed against DDW (Spectrapor 3 dialysis tubing). Small aliquots were hydrolyzed in 6 N HCl for 24 h at 110°C and their amino acid concentrations were determined (Dionex BIOLC) using ninhydrin detection.

Epitaxial Overgrowth

Synthetic calcite crystals were grown by slow diffusion of $(NH_4)_2CO_3$ vapor into 10 mM calcium chloride solution containing cleaned spicules. The epitaxially overgrown specimens were then lightly rinsed with DDW and dried. Under these conditions macromolecules are released from the spicules and induce morphological changes on the overgrown crystals. These were examined in the SEM after coating with gold. For more details, see ref 8.

Synchrotron X-Ray Diffraction Measurements

Selected individual spicules were glued to thin glass fibers in different orientations to eliminate a possible effect of their position relative to the beam on crystal texture. They were attached to brass pins. Determination of the orientation matrix and preliminary measurements were performed on a Rigaku rotating Cu-anode four-circle diffractometer equipped with a Siroflux double monochromator condensing-collimating system. As calcite crystals are extremely ordered, their fine textural parameters are beyond the resolution of standard X-ray equipment. High-resolution diffraction peak profiles were therefore collected using well-collimated synchrotron X-radiation at the Brookhaven National Laboratory, National Synchrotron Light Source (line X7B), Upton, N.Y. Separate determinations of the coherence lengths and angular dispersions were achieved by measuring the specific diffraction peaks in the $\omega/2\theta$ and ω scan modes, respectively, with a Ge(220) analyzer crystal introduced on the detector arm of the six-circle Huber diffractometer. For a description of the experimental setup, see ref 10. To study the crystal imperfections in different crystallographic directions, and even within a set of symmetry related directions, three crystallographically equivalent reflections were measured for each of the following {*hkl*}-families[2]: {104}, {018}, {0 0 12}, {006}, {110}, {030}, {202}, and for several crystals also {024}, {012}, {113}, {1 0 10}, {116}, {1 1 12}. Each profile consisted of 100 data points. For the triradiates and curved monaxons, steps of 0.004 and 0.002° for the ω and $\omega/2\theta$ scans, respectively, were used, and 0.0005 and 0.001°, respectively, for the highly ordered synthetic calcite crystal and the slender monaxons.

Treatment of Data

The crystal texture was characterized by two parameters. The coherence length (CL) was calculated by application of the Scherrer formula (19) to the diffraction peak 2θ width measured in the $\omega/2\theta$ scan mode:

$$CL = \frac{\lambda}{\cos\theta \sqrt{B^2_{\omega/2\theta} - \beta^2}},$$

where λ is the wavelength, θ is the Bragg angle, and β is the instrumental resolution, expressed in radians. In our setup, λ = 0.9195 Å and β = 0.003°. The peak width, $B_{\omega/2\theta}$ (in radians), was determined from the integrated intensity of the peak divided by its maximum intensity after subtracting the background level. In the ω scan mode, the peak width at half height corresponds to the average angular spread of the domains. The reciprocal of the angular dispersion was used as a measure of the degree of alignment of the domains in a given direction ($A = B_\omega^{-1}$). The discrepancy factor *R* was evaluated by comparing each value in one set of reflections with the corresponding value in a parallel set and then calculating the mean deviation for the entire ensemble of pairs. Magnesium contents were determined from the reduction in the calcite cell dimensions (20).

RESULTS

A series of diffraction peak profiles in the ω and $\omega/2\theta$ scan modes were collected for one pure calcite crystal, three *Clathrina* triradiates, two *Sycon* slender monaxons, and three *Sycon* curved monaxons. The coherence lengths were estimated by application of the Scherrer formula to the peak widths measured in the $\omega/2\theta$ mode in each crystallographic direction (19). The reciprocal of the peak width in the ω scan mode was used as a measure of the degree of alignment of the mosaic blocks in a given direction. The textural characteristics of each spicule were then reconstructed by plotting the deduced values of the coherence lengths and alignments in all the measured crystallographic directions. The coherence lengths and degrees of alignment for selected representative sections are shown (see Figs. 2 through 5). The relations of these planes to the crystal morphology are also shown. Data are presented from only one of the several crystals of each type examined. Each point represents the extremity of a vector, lying in the section and originating at the center of the plot, whose length is proportional to the coherence length (upper plots) or to the degree of alignment (lower plots). The vector direction is coincident with the diffraction vector of the corresponding crystallographic plane. The calculated discrepancy factors between the textural parameters of the spicules within each group, *R*, are reported in the figure legends for both modes of measurement.

Synthetic calcite crystal

The diffraction peak widths for the synthetic calcite crystal are all close to the resolution limit of the instrument. Thus, the crystalline domains are very large, with the average coherence length being about 8000 Å (**Fig. 2*A***). They are also highly aligned, with the average degree of alignment being 180 degrees^{-1} (Fig. 2*B*). The crystal is texturally almost isotropic. However, there is a characteristic average coherence length for each set of crystallographically equivalent directions. This may be due to the empirical character of the Scherrer formula that does not yield constant values for different values of the Bragg angles and/or to real intrinsic differences in the crystal texture in different directions. The average values for each set of planes were used as reference in the study of the textural anisotropies of the biogenic crystals.

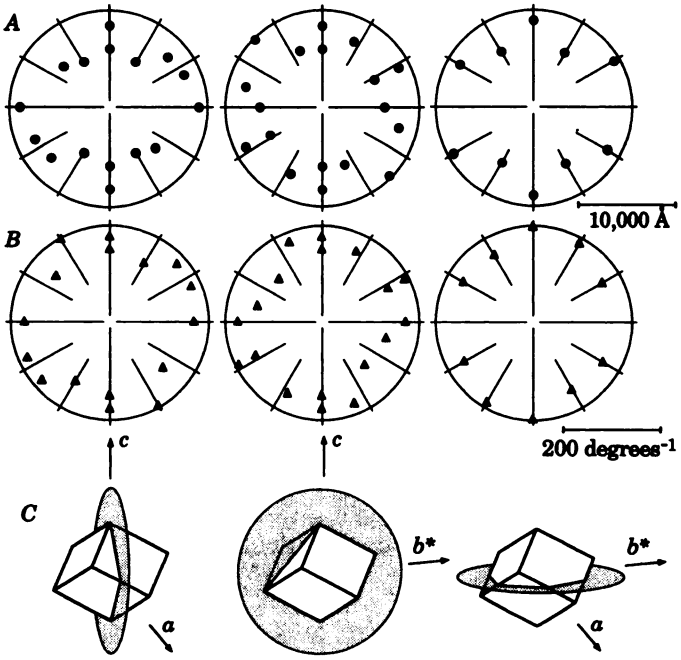

Figure 2. Measured textural parameters of a synthetic calcite crystal. *A)* Measured coherence lengths in the *ac* plane (left), *cb** plane (center), and *ab** plane (right). Each point represents the extremity of a vector originating at the center of the plot and whose length is proportional to the coherence length in the corresponding crystallographic direction. In the [001] and [012] directions, two reflections at different Bragg angles were measured [(006) and (0 0 12), (012) and (024), respectively]. *B)* Measured degrees of alignment. The sections and the representations are as in *A*. *C)* Morphology of a synthetic calcite crystal showing the orientations of the sections represented in *A* and *B*.

Sycon slender monaxon

The textural characteristics of the slender monaxon, for which a set of 21 reflections was collected, are shown in **Fig. 3** for sections in the *ca* and *cb** planes. The average coherence length is 6000 Å, and the domains are almost isotropic in all crystallographic directions (Fig. 3*A*). There is only a slight elongation, if any, of the domains in the *c* direction. The average degree of alignment is 110 degrees^{-1} (Fig. 3*B*). The textural parameters of the slender monaxons are therefore similar to those of the synthetic calcite crystal. The magnesium content is undetectable based on unit cell dimensions. Slow epitaxial overgrowth of calcite crystals on the spicule substrate showed no morphological changes in the synthetic crystals, suggesting that little or no protein is present within the spicule (Fig. 1*C*, insert).

Clathrina triradiate spicule

Figure 4 shows the textural parameters of a *Clathrina* triradiate spicule, for which a set of 26 reflections was collected. Sections in the *cb** and *ab** planes are presented. The domains are significantly smaller than those of the control calcite crystal. The average domain size is 1900 Å. The coherence length is reduced along the *c* axis compared with the *b** axis (Fig. 4*A*). The average perfect domain thus has a shape of a disc flattened in the *c* direction. It resembles the overall morphology of the spicule to the extent that the growth of the spicule is restricted along the *c* axis relative to the *ab* plane (Fig. 4*C*). The average alignment of the domains is drastically decreased compared to the pure calcite crystal (A = 16 degrees^{-1}), and is roughly the same in all crystallographic directions (Fig. 4*B*). It is noteworthy that the integrated intensity of the diffracted beam accounts for only about 20% of the expected value for an equivalent volume of synthetic calcite crystal, possibly implying that a significant proportion of the spicule is amorphous. The magnesium content in the crystalline part is 16 mol %, and the intracrystalline protein content is 0.1 wt %.

Sycon curved monaxon

Figure 5 shows the textural parameters of the curved monaxon for which a data set of 39 reflections was collected. One section almost perpendicular to the morphological axis, *ca*, and two parallel to the morphological axis, defined by *c*, *b**, and *a*, [012] directions, respectively, are presented. In the ca plane, the coherence lengths and degrees of alignment are almost isotropic, irrespective of the crystallographic orientation. Within this plane, the average coherence length is 1300 Å (Fig. 5*A*, left), and the average degree of alignment is 14 degrees^{-1} (Fig. 5*B*, left). Both values are significantly reduced compared to those of the synthetic calcite crystal. In the planes parallel to the morphological axis, the coherence

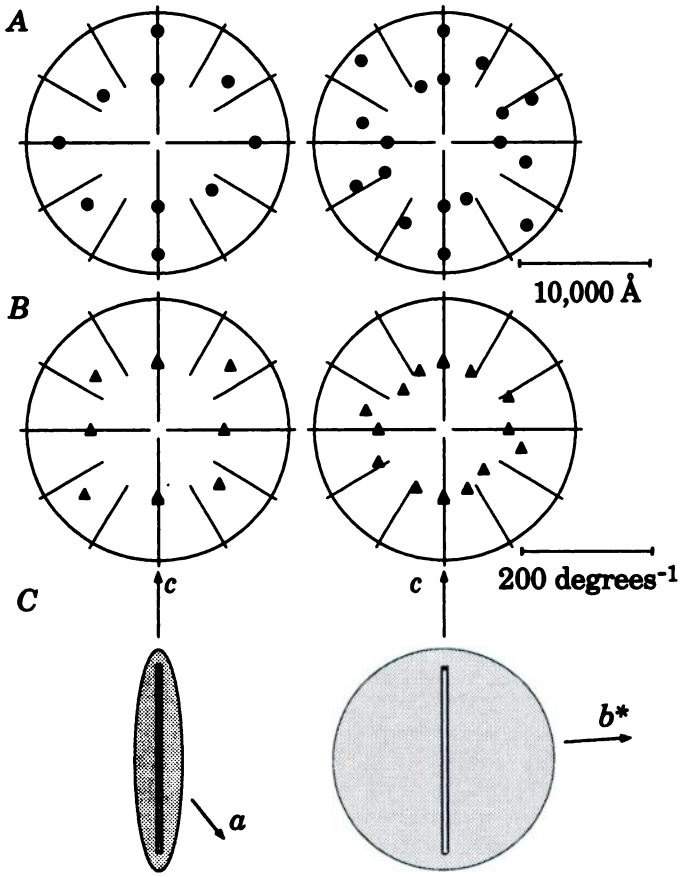

Figure 3. Measured textural parameters of a *Sycon* slender monaxon in the *ac* and *b*c* planes. The representation is as in Fig. 2. *A)* Measured coherence lengths. *B)* Measured degrees of alignment. *C)* Morphology of the spicule showing the orientations of the corresponding sections. The discrepancy *R* factors between the two measured spicules are 11.7% and 11.3% for coherence length and degree of alignment, respectively.

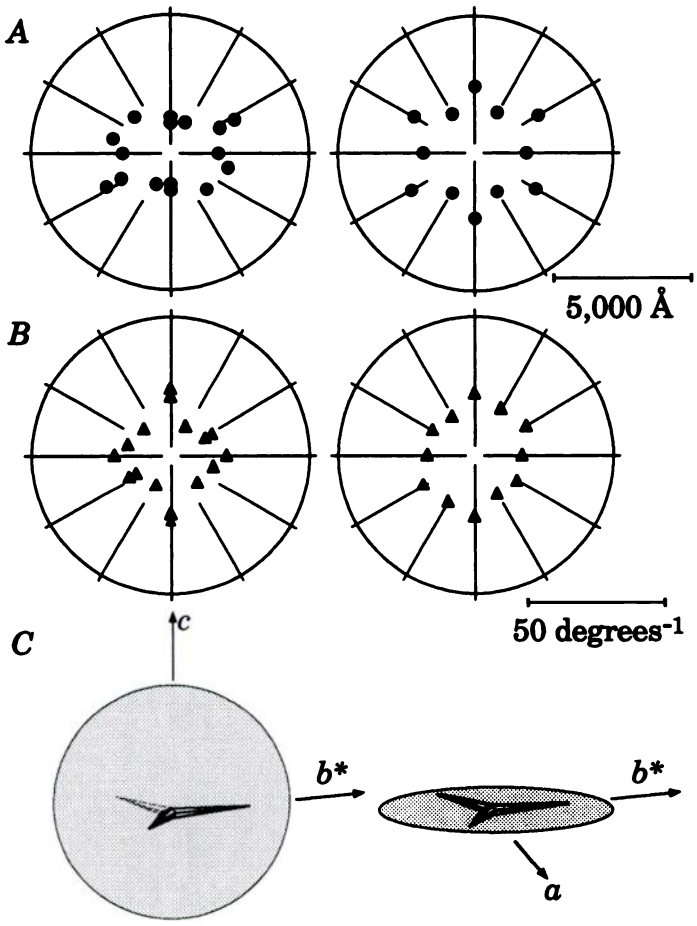

Figure 4. Measured textural parameters of a *Clathrina* triradiate spicule in the *ac* and *ab** planes. The representation is as in Fig. 2. *A)* Measured coherence lengths. *B)* Measured degrees of alignment. *C)* Morphology of the spicule showing the orientations of the sections represented in *A* and *B*. The discrepancy *R* factors between the three measured spicules are 9.5% and 19.6% for coherence length and degree of alignment, respectively.

lengths and degrees of alignment show marked anisotropy, with the maxima being well aligned with the morphological spicule axis (Fig. 5*C*). The absolute maxima values are similar to those of synthetic calcite. A most remarkable observation is that in both modes of measurement, the widths of one peak in each family of symmetry-related reflections were systematically different from the other two. In all cases the larger coherence lengths or greater degree of alignment were between the planes more or less perpendicular to the spicule morphological axis. This is illustrated for the {012} family of reflections, for which the largest differences were observed, in a 3-dimensional plot of the vectors of all the coherence lengths for this crystal (Fig. 5*D*). The magnesium content is 11.5 mol %, and the intracrystalline protein content is 0.08 wt %.

DISCUSSION

Analysis of the coherence lengths and degrees of alignment shows that the texture of the *Sycon* slender monaxons closely resemble that of synthetic calcite, whereas the textures of the *Sycon* curved monaxons and the *Clathrina* triradiates differ from each other and from pure calcite.

As the calculated values of the coherence lengths for the synthetic calcite crystal are not completely isotropic, we have normalized the coherence length measurements of each spicule to those of control calcite crystal (**Fig. 6**). The normalization should take into account any deviations due either to the intrinsic nature of the calcite structure or to the calculations. We then used the values obtained to reconstruct a 3-dimensional envelope of all the normalized coherence length vector extremities of each spicule. These represent visually the deviation of the perfect domain shape from that of the synthetic calcite. It can be appreciated that the variations between spicules of the same type are rather small (the calculated discrepancy factors, *R*, are less than 12%). In fact, they are much smaller than the observed anisotropy factors as well as the variations between different spicule types.

We now consider the results obtained in relation to the initial hypothesis, that there is a correspondence between protein intercalation, textural anisotropy, and the macroscopic morphology of the spicule. We stress that were the macro-

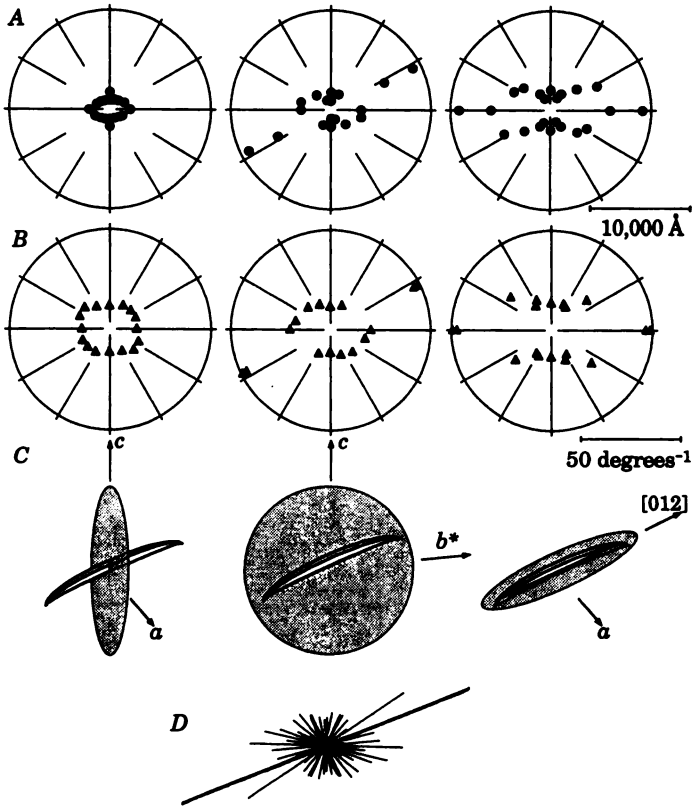

Figure 5. Measured textural parameters of a *Sycon* curved monaxon spicule. One section is in the *ca* plane almost perpendicular to the morphological axis (left), and two sections are parallel to the morphological axis. They are defined by *c*, *b** (center), and *a*, [012] directions (right). The representation is as in Fig. 2. *A)* Measured coherence lengths. *B)* Measured degrees of alignment. *C)* Morphology of the spicule showing the orientations of the corresponding sections. *D)* Three-dimensional representation of the coherence lengths in all the measured crystallographic directions. The vectors of the symmetry related reflections (012), ($\bar{1}02$), and ($1\bar{1}2$)[2] are in bold. The discrepancy *R* factors between the three measured spicules are 9.9% and 11.1% for coherence length and degree of alignment, respectively.

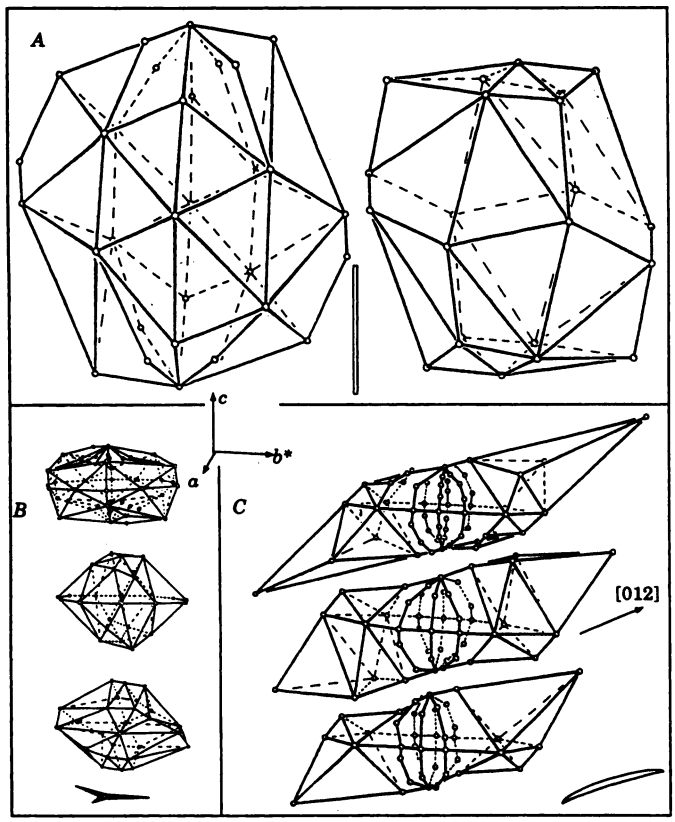

Figure 6. Reconstructed 3-dimensional shapes of the average perfect domains in the measured spicules, all drawn to the same scale. Each point represents the extremity of a vector originating at the center of the plot and whose length is proportional to the coherence length in a defined crystallographic direction, normalized to the corresponding value measured for the synthetic calcite crystal. To generate the envelope, each point was arbitrarily connected to some of the nearest neighbors. For comparison, the morphologies of the whole spicules are shown in the same orientations. *A)* The two *Sycon* slender monaxon spicules. *B)* The three *Clathrina* triradiate spicules. *C)* The three *Sycon* curved monaxons.

scopic morphology of the crystal determined exclusively by external physical constraints, an isotropic texture would be expected, such as that of synthetic calcite.

In contrast to expectations, the slender monaxons indeed have isotropic coherence length values, notwithstanding their highly elongated morphology (Fig. 6*A*). The textural analyses of the slender monaxons are so similar to that of the synthetic calcite crystal that it is unlikely that occluded proteins are present within the spicule. Unfortunately, too little material was available to demonstrate this directly by amino acid analysis. The facts that the spicules cleave on the normal {104} cleavage planes and not conchoidally, and that the slowly overgrown crystals expressed only the stable {104} faces (Fig. 1*C*, insert), both support the notion that intracrystalline proteins are absent. We surmise, therefore, that the unusual shape of the spicule is achieved entirely by some external means. It is not due to occlusion of proteins or other ions inside the growing crystal that would reduce growth in some directions relative to others. In contrast to most other calcisponge spicules, the slender monaxons are very fragile, contain no magnesium, protrude almost entirely from the tissue, and are concentrated around the osculum. It would be interesting to know how the material properties of these spicules may be adapted to their function.

The *Clathrina* triradiates contain intracrystalline proteins (0.1 wt %). They also cleave with conchoidal fracture, suggesting that the intracrystalline proteins alter their mechanical properties. There is strong evidence to support the fact that their textural properties are determined at least in part by the presence of occluded proteins on specific planes within the crystals. Both the overgrowth experiments and the experiments in which calcite crystals are grown de novo in a solution containing extracted intracrystalline proteins show that some of these proteins preferentially interact with the {001} planes of calcite (8). This corresponds well with the observation that the reconstructed average shape of the perfect domain is a disc flattened in the *c* axis direction and isotropic in the *ab* plane (Fig. 6*B*). The discs are slightly misoriented in all directions with respect to one another. We note that the coherence length in the *ab* plane is also smaller than in synthetic calcite, implying protein interference on these planes as well. The triradiate shape of the spicule does require limitation of growth in all directions, excluding a^*, along which each arm grows. As the three arms form an angle of 120° with each other, the average effect on the three directions generates pseudoisotropy in the plane.

The *Sycon* curved monaxons also contain protein (0.08 wt %), and cleave with conchoidal fracture. Overgrowth experiments on these spicules show that new faces develop both perpendicular to and roughly parallel to the *c* axis (Fig. 1*D*, insert). This, too, is consistent with the reconstructed shape of the average perfect domain, which is roughly a cylinder elongated in a direction oblique to the *c* axis (Fig. 6*C*). Analysis of the textural measurements of the *Sycon* monaxons shows that the correspondence between the shape of the perfect domains and the macroscopic morphology is much superior to what would be expected only on the basis of recognition of specialized proteins for selected crystallographic planes. These spicules were selected for study because their morphology does not reflect the hexagonal symmetry of calcite. We therefore suspected that if protein intercalation is indeed related to the modulation of morphology, differences in coherence lengths would be observed within families of symmetry related reflections. By measuring the peak profiles of several families of such reflections, we found that in each case one reflection differed in width from the other two, and that this difference was clearly related to spicule morphology. The {012} family of reflections[2] is of particular interest, because one of its members, (012), is well aligned with the spicule morphological axis but the other two, ($\bar{1}02$) and ($1\bar{1}2$), form an angle of about 60° with the spicule axis. The coherence length in the [012] direction is 8200 Å, in comparison to 1800 and 1900 Å in the other two directions. We stress that symmetry-related reflections correspond to planes of identical structure in the crystal, related in the case of calcite, by hexagonal symmetry around the *c* axis (21). As all these crystal planes are identical in structure, the differences in textural properties cannot be accounted for by specific protein-crystal interactions alone or, for that matter, by specific magnesium-crystal interactions. Any such interaction would be identical for all the family of symmetry-related planes in an isotropic environment. We must conclude that within the space where the spicule is formed and the proteins are introduced, the organism creates an anisotropic environment. This is tantamount to stating that there is almost perfectly orchestrated control over the microenvironment of crystal growth.

We note that the degree of alignment between the perfect domains is also anisotropic, with a much higher degree of alignment along the morphological axis than oblique to it, irrespective of the crystallographic symmetry. The resulting

model obtained by combining the coherence length and alignment is a crystal built of cylindrical domains with their axes almost perfectly aligned, and slightly rotating azimuthally around their long axes. This would suggest that the proteins are somehow introduced in such a way that they are preferentially aligned with the spicule axis.

We can envisage several scenarios that may account for these observations, such as oriented nucleation of the crystal coupled with unidirectional growth or highly specific introduction of the interacting macromolecules into the crystal growth microenvironment. The former scenario would result in only a subset of the identical faces being available for interaction from solution by macromolecules, whereas the latter scenario invokes an external mechanism for targeting the macromolecules to some sites on the crystal surface and not others. Clearly, we need to know much more about biological crystal growth and the microenvironment in which this occurs in order to better understand these most enigmatic observations. FJ

We thank Dr. Felix Frolow and Yarek Majewski of the Weizmann Institute for their help in setting up the Siroflux system, and Ivan Kuzmenko for help with the graphic programs. S. W. is the incumbent of the I. W. Abel Professorial Chair of Structural Biology, and L. A. is the incumbent of the Patrick E. Gorman Professorial Chair of Biological Ultrastructure. This study was funded in part by the Kimmelman Center for Biomolecular Structure and Assembly, and by grant no. 92-00100 from the U.S.-Israel Binational Science Foundation. The research was carried out at Brookhaven National Laboratory under contract DE-AC02-76CH00016 with the U.S. Department of Energy and supported by its Division of Chemical Sciences, Office of Basic Energy Sciences.

Note added in proof. The authors wish to note the following work: Aizenberg, J., Hanson, J. Koetzle, T. F., Leiserowitz, L., Weiner, S., and Addadi, L. (1995) Biologically induced reduction in symmetry: a study of crystal texture of calcitic sponge spicules. *Chemistry - A European J.*, submitted.

REFERENCES

1. Simkiss, K. (1986) The processes of biomineralization in lower plants and animals—an overview. In *Biomineralization in Lower Plants and Animals* (Leadbeater, B. S. C., and Riding, R., eds) pp. 19-37, Clarendon Press, Oxford
2. Simkiss, K., and Wilbur, K. M. (1989) *Biomineralization. Cell Biology and Mineral Deposition,* Academic, San Diego
3. Lowenstam, H. A., and Weiner, S. (1989) *On Biomineralization,* Oxford University Press, New York
4. Mann, S. (1989) Crystallochemical strategies in biomineralization. In *Biomineralization. Chemical and Biochemical Perspectives* (Mann, S., Webb, J., and Williams, R. J. P., eds) pp. 189-222, VCH Publishers, Weinheim
5. Weiner, S., and Addadi, L. (1991) Acidic macromolecules of mineralized tissues. *Trends Biochem.* **16,** 252-256
6. Berman, A., Addadi, L., and Weiner, S. (1988) Interactions of sea urchin skeleton macromolecules with growing calcite crystals—a study of intracrystalline proteins. *Nature* **331,** 546-548
7. Albeck, S., Aizenberg, J., Addadi, L., and Weiner, S. (1993) Interactions of various skeletal intracrystalline components with calcite crystals. *J. Am. Chem. Soc.* **115,** 11691-11697
8. Aizenberg, J., Albeck, S., Weiner, S., and Addadi, L. (1994) Crystal-protein interactions studied by overgrowth of calcite on biogenic skeletal elements. *J. Cryst. Growth* **142,** 156-164
9. Berman, A., Addadi, L., Kvick, Å., Leiserowitz, L., Nelson, M., and Weiner, S. (1990) Intercalation of sea urchin proteins in calcite: study of a crystalline composite material. *Science* **250,** 664-667
10. Berman, A., Hanson, J., Leiserowitz, L., Koetzle, T. F., Weiner, S., and Addadi, L. (1993) Biological control of crystal texture: a widespread strategy for adapting crystal properties to function. *Science* **259,** 776-779
11. Addadi, L., Aizenberg, J., Albeck, S., Berman, A., Leiserowitz, L., and Weiner, S. (1994) Controlled occlusion of proteins: a tool for modulating the properties of skeletal elements. *Mol. Cryst. Liquid Cryst. Sci. Technol.* **248,** 185-198
12. Minchin, E. A. (1898) Materials for a monograph of the *Ascons.* I. On the origin and growth of the triradiate and quadriradiate spicules in the family *Clathrinidae. Q. J. Microsc. Sci.* **40,** 469-587
13. Haeckel, E. H. P. A. (1872) *Die Kalkschwämme.* G. Reimer, Berlin
14. Ledger, P. W. (1975) Septate junctions in the calcareous sponge *Sycon ciliatum. Tissue & Cell* **7,** 13-18
15. Jones, W. C., and Jenkins, D. A. (1970) Calcareous sponge spicules: a study of magnesian calcites. *Calcif. Tiss. Res.* **4,** 314-329
16. Jones, W. C. (1970) The composition, development, form and orientation of calcareous sponge spicules. *Symp. Zool. Soc. Lond.* **25,** 91-123
17. Jones, W. C. (1955) Crystalline properties of spicules of *Leucosolenia complicata. Q. J. Microsc. Sci.* **96,** 129-149
18. Tsurnamal, M. (1975) The calcareous sponges of shallow habitats along the Mediterranean Coast of Israel. *Israel J. Zool.* **24,** 137-153
19. Guinier, A. (1963) *X-Ray Diffraction in Crystals, Imperfect Crystals, and Amorphous Bodies.* W. H. Freeman and Co., San Francisco
20. Goldsmith, J. R., Graf, D. L., and Heard, H. C. (1961) Lattice constants of the calcium-magnesium carbonates. *Am. Mineralogist* **46,** 453-457

Received for publication September 6, 1994.
Accepted for publication September 29, 1994.